Asian Journal of Chemistry; Vol. 26, No. 13 (2014), 4140-4142

ASIAN JOURNAL OF CHEMISTRY

http://dx.doi.org/10.14233/ajchem.2014.17733

Magnetic Properties of Arrays of Nickel Nanowires Embedded in Alumina Nanoholes†

CHUL KYU SONG[1,2], DHA-HAE KIM[1], SO-YEON YOO[1], SE-NA JANG[1] and SEUNG HUN HUH[1,*]

[1]Nanotechnology Convergence Lab, Korea Institute of Ceramic Engineering and Technology, Seoul 153-801, Republic of Korea
[2]Department of Materials Science and Engineering, Korea University, Anam-dong, Seoul 136-713, Republic of Korea

*Corresponding author: Fax: +82 2 32827769; Tel: +82 2 32827820; E-mail: shhuh@kicet.re.kr

Published online: 23 June 2014; AJC-15428

Arrays of nickel nanowires were produced by electrochemical deposition of nickel ions onto the array of alumina nanoholes. The diameter and length of the nickel nanowires are 70-80 and 3-7 mm, respectively. The nickel nanowires had ferromagnetism and shape anisotropy to the parallel and perpendicular direction. Importantly, only parallel direction of nickel nanowires has drastic change of coercivities at 50 K, which is different from the reported result. Phase-transition like behaviour at 50 K is explained by three factors of magnetoeleastic effect, degree of thermal fluctuation of magnetic spin moments and shape anisotropy.

Keywords: Nickel nanowire, Alumina template, Magnetoelastic, Nanomagnetism.

INTRODUCTION

Ferromagnetic nanowires have attracted much attention in recent years because they exhibit a high ratio of remanence to saturation magnetization (M_r/M_s) due to the shape anisotropy[1-8]. The high M_r/M_s ratio can remain less than 10 nm in diameter[2,4] and thus the ferromagnetic nanowires are expected to be suitable for the high-density perpendicular magnetic recording[1-7]. A regular ferromagnetic nanowires array can be fabricated by electrochemical deposition of metallic ions onto an anodic alumina template with self-assembled nanoholes[1-7]. In this case, the most of 3-*d* ferromagnetic nanowires (Fe, Co and Ni) have shown the excellent magnetic properties compared to the corresponding bulks[1-8]. However, the recent report has shown the poor magnetic properties for only nickel nanowires with decreasing temperature[9-11]. For examples, the decreasing coercivity (H_c) and remanence ratio with decreasing temperature[9-11]. This is due to the magnetoelastic effects; a large mismatch of the thermally induced contraction between the nickel nanowires and the alumina template in the cooling process[9-11]. This explanation is based on the Dubois *et al.'s* experiment that they shows a direct evidence for the magnetoelastic effects by using the X-ray diffraction; the bond length of the nickel nanowires contracts of 2.5 % in polycarbonate membranes as temperature decreased from 300 to 100 K[12]. This effect might be natural considering that the bulk Ni showed the most prominent magnetostriction in the 3-*d* ferromagnetic metals under tensile or compressive stress[13]. However, In one-dimensional Ni system, the magnetostriction or magnetoelastic effect may become more complex because of the matter of shape anisotropy[1-12] and thermal fluctuation of spin-spin coupling.

In this study, array of nickel nanowires embedded in anodic alumina template were produced and their magnetism were closely investigated in the temperature range of 300-2 K. Based on the plots of H_c according to temperature, phase-transition like behaviour at 50 K was observed for the only parallel direction of nickel nanowires. This is explained by three effects of compression stress of Ni crystals (magnetoeleastic effect), degree of thermal fluctuation of Ni spins and shape anisotropy. From here, the subscript // and ⊥ means the parallel- and perpendicular-direction to the long axis of Ni NRs, respectively.

EXPERIMENTAL

Alumina template with self-assembled nanohole arrays was prepared *via* a two-step anodization process[14,15]. The degreased aluminum substrate (99.999 %) was electrochemically polished in a mixture solution of perchloric acid and ethanol (1:4 in volume). The first anodization was conducted for 24 h at 20 ºC in a 0.3 M oxalic acid solution and then the oxide layer was removed. The regular hexagonal nanohole arrays were prepared after the second anodization for 1 h at 2 ºC. The constant voltage of DC 40 V and a platinum counter electrode were used. With the Watts bath consisting of 300 g/L $NiSO_4 \cdot 6H_2O$, 45 g/L $NiCl_2 \cdot 6H_2O$ and 45 g/L H_3BO_4[15], the nickel nanowire arrays were fabricated by the electrochemical deposition of Ni ions onto the nanohole array by applying

†Presented at 5th International Symposium on Application of Chemical and Analytical Technologies in Nuclear Industries (Nu-ACT 2013), Daejeon, Korea

constant voltage of AC 10-15 V. Their morphologies and magnetic properties were characterized with a field emission scanning electron microscope (FE-SEM) and superconducting quantum interference device (SQUID), respectively.

RESULTS AND DISCUSSION

Fig. 1(a) and (b) shows the FE-SEM images for the top and the section view of alumina template with self assembled nanohole array, respectively. Pore length and diameter of alumina nanohole is 70-80 nm and 6-7 μm, respectively. The alumina nanoholes (Fig. 1(b)) are filed with Ni during electrochemically deposition and then white spots due to filling over of Ni (Fig. 1(d))) are observed on the surface of alumina (Fig. 1(c)). The filling ratio is estimated to be 50-100 % based on Fig. 1(e), indicating that the nickel nanowires are 3-7 μm in length. Fig. 1(f) shows a good array of nickel nanowires with 70-80 nm in diameter. Aspect ratio (length to diameter) of nickel nanowires is 45-100.

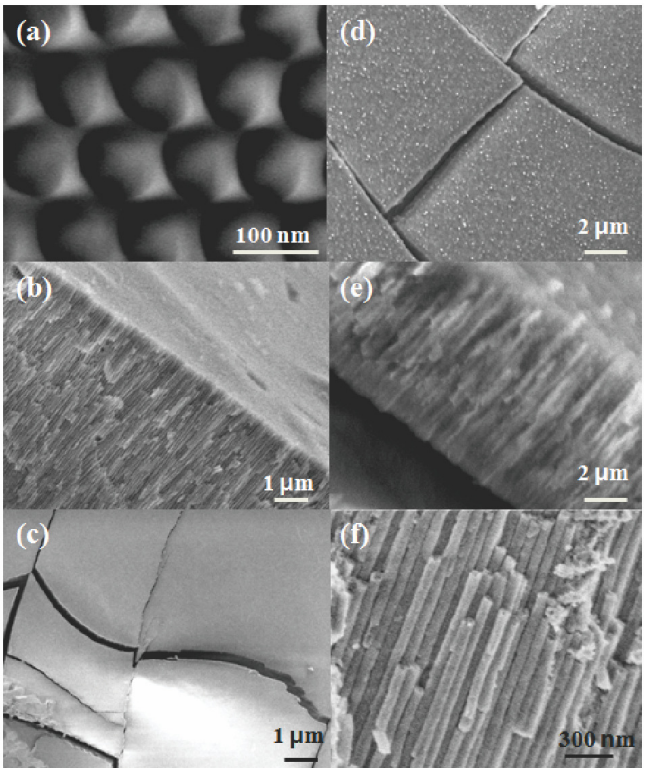

Fig. 1. FE-SEM images of surface and section views for the array of alumina nanoholes (a-c) and the surface and section views for the array of nickel nanowires embedded in alumina template (d-f)

Figs. 2 and 3 show the magnetic hysteresis loops for the parallel (//) and perpendicular direction (⊥) of the nickel nanowires at 300 and 2 K, respectively. At 300K, $H_{c//}$, $M_{r//}$, $M_{s//}$ and $M_{r//}/M_{s//}$ is 598 Oe, 4.2y × 10^{-3} emu, 4.7y × 10^{-3} emu and 0.84, respectively. At 300 K, $H_{c\perp}$, $M_{r\perp}$, $M_{s\perp}$ and $M_{r\perp}/M_{s\perp}$ is 239 Oe, 0.67y × 10^{-4} emu, 3.7y × 10^{-3} emu and 0.18, respectively. At 2K, $H_{c//}$, $M_{r//}$, $M_{s//}$ and $M_{r//}/M_{s//}$ is 276 Oe, 1.7y × 10^{-3} emu, 4.9y × 10^{-3} emu and 0.35, respectively. At 2 K, $H_{c\perp}$, $M_{r\perp}$, $M_{s\perp}$ and $M_{r\perp}/M_{s\perp}$ is 365 Oe, 2.5y × 10^{-3} emu, 4.5y × 10^{-3} emu and 0.56, respectively. These results are summarized in Table-1.

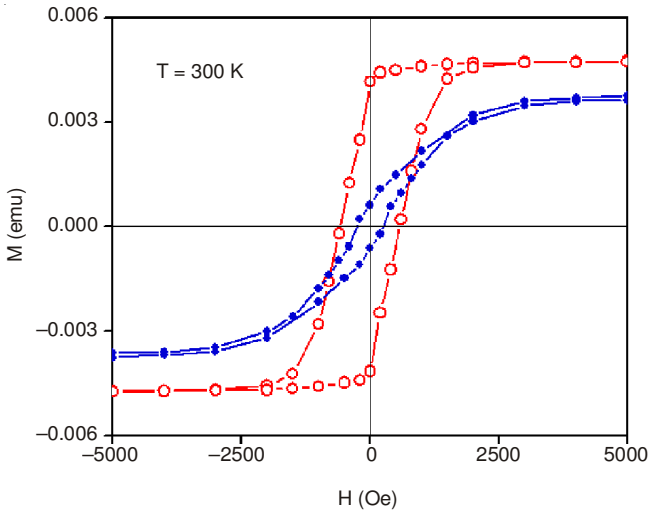

Fig. 2. Hysteresis loops for the parallel (red lines) and perpendicular direction (blue lines) for the nickel nanowires at 300 K

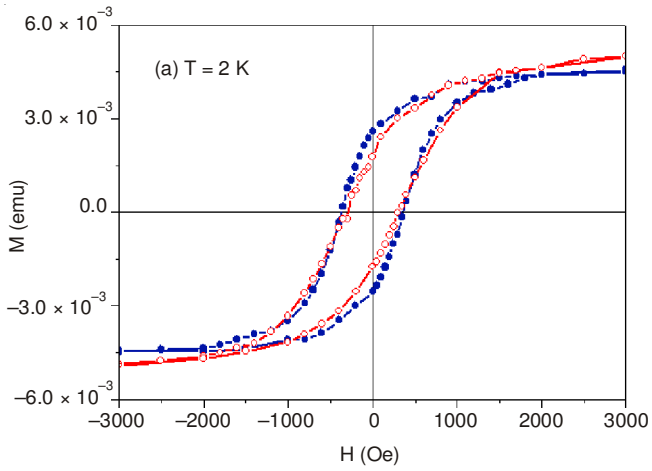

Fig. 3. Hysteresis loops for the parallel (red lines) and perpendicular direction (blue lines) for the nickel nanowires at 2 K

TABLE-1
REMANENCE (M_r) AND SATURATION MAGNETIZATION (M_s) FOR THE PARALLEL (//) AND PERPENDICULAR DIRECTION (⊥) TO THE NICKEL NANOWIRES AT 300 AND 2 K

Temp. (K)	$M_{r//}$	$M_{r\perp}$	$M_{s//}$	$M_{s\perp}$	$M_{r//}/M_{s//}$	$M_{r\perp}/M_{s\perp}$
	(× 10^{-3} emu[a])		(× 10^{-3} emu[a])			
300	4.2[b]	0.67[b]	4.7[b]	3.7[b]	0.84[c]	0.18[c]
2	1.7	2.5	4.9	4.5	0.35	0.56

[a]emu: amounts of Ni NWs embedded in alumina template were not analyzed (not emu/g). [b]Error: ± 0.1 × 10^{-3} emu. [c]Error: ± 0.02.

At 300 K, $H_{c//}$, $M_{r//}$ and $M_{r//}/M_{s//}$ are superior to corresponding $H_{c\perp}$, $M_{r\perp}$ and $M_{r\perp}/M_{s\perp}$ because of shape anisotropy: long axis of ferromagnetic nanowire is easy to magnetize[13]. However, at 2 K, $H_{c\perp}$, $M_{r\perp}$ and $M_{r\perp}/M_{s\perp}$ become larger than $H_{c//}$, $M_{r//}$ and $M_{r//}/M_{s//}$. This is unusual tendency. In general, $H_{c//}$, $M_{r//}$ and $M_{r//}/M_{s//}$ are all increased as decreasing temperature and superior to corresponding $H_{c\perp}$, $M_{r\perp}$ and $M_{r\perp}/M_{s\perp}$ due to both effects of shape anisotropy and suppression of thermal fluctuation of magnetic spin moments. In this experiment, the unusual magnetic properties can be explained by magnetoeleastic effects[9-11]. Fig. 4 is the plot of $H_{c//}$ and $H_{c\perp}$ according to cooling temperature (Table-2). Importantly, phase-transition-like behaviour of $H_{c//}$ at 50 K (T_c) is observed and there is crossover

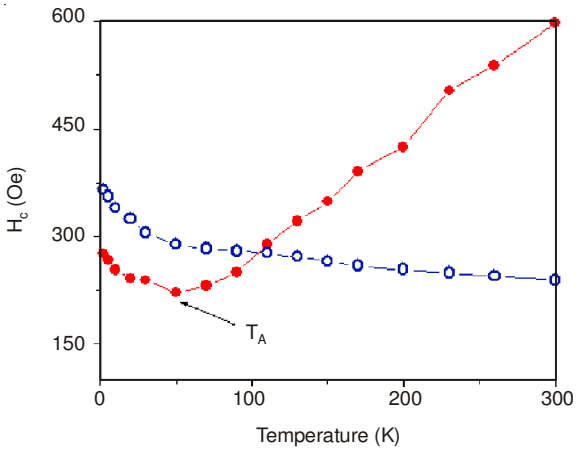

Fig. 4. Plots of H_c for the parallel (red dots and line) and perpendicular direction (blue circles and line) of the nickel nanowires in the temperature range of 300-2 K. Inserts are the magnified plots

TABLE-2
TEMPERATURE-DEPENDENT COERCIVITIES (H_c) FOR THE PARALLEL (//) AND PERPENDICULAR DIRECTION (⊥) TO THE NICKEL NANOWIRES

Temperature (K)	$H_{c//}$	$H_{c\perp}$	K	$H_{c//}$	$H_{c\perp}$
2	276[a]	365[a]	110	289	277
5	267	356	130	321	272
10	253	340	150	349	265
20	242	325	170	391	259
30	239	305	200	425	254
50	222	289	230	504	249
70	231	283	260	539	245
90	250	280	300	598	239

[a]Error: ± 2 Oe.

temperature of T_c that the $H_{c\perp}$ become larger than the $H_{c//}$ at 100 K. This cannot be simply explained by using a mageto-elastic factor, but a combinatorial effect of compressive stress, thermal fluctuation and shape anisotropy.

Nickel nanowires are compressed owing to alumina contraction as decreasing temperature[9-12] and then their magnetic spins (//) to be spin-spin coupled gradually. Thus, $H_{c//}$, $M_{r//}$, $M_{r//}/M_{s//}$ are all decreased due to magnetoelastic effects as decreasing temperature. In the meanwhile, thermal fluctuation becomes suppressed gradually as decreasing temperature: thus, cooling effect and shape anisotropy (//) have a tendency to enhance magnetic spin moments and spin-spin coupling. Therefore, for the parallel direction (//) below the critical temperature, the coupled effects with suppressing the thermal fluctuation and shape anisotropy can overcome the magneto-elastic factor. In this experimental condition, the critical temperature is 50 K. Although the values of $H_{c//}$ are drastically increased below 50 K, those of $H_{c\perp}$ are always larger than those of $H_{c//}$ below 100 K. This indicates that the degree of thermal fluctuations of magnetic spin moments to the perpendicular direction (⊥) is the most outstanding factor below 100 K.

Conclusion

Magnetic properties of array of nickel nanowires stressed by alumina template were detailed in this experiment. Plots of temperature-dependent coercivities showed phase-transition-like behaviour for the $H_{c//}$ at T_c of 50 K and crossover temperature for $H_{c\perp}$ (larger than $H_{c//}$) below 100 K. This indicates that one-dimensional magnetic materials embedded in different materials should be explained by three factors of magneto-elastic effect, shape anisotropy and thermal fluctuation of magnetic spin moments according to the temperature changes.

ACKNOWLEDGEMENTS

This work was supported by the Development Program of "Graphene coating materials for electromagnetic interference shielding" through the Ministry of Trade, Industry & Energy (MOTIE 10044380).

REFERENCES

1. T.M. Whitney, P.C. Searson, J.S. Jiang and C.L. Chien, *Science*, **261**, 1316 (1993).
2. H. Zeng, R. Skomski, L. Menon, Y. Liu, S. Bandyopadhyay and D.J. Sellmyer, *Phys. Rev. B*, **65**, 134426 (2002).
3. K. Nielsch, R.B. Wehrspohn, J. Barthel, J. Kirschner, U. Gösele, S.F. Fischer and H. Kronmüller, *Appl. Phys. Lett*., **79**, 1360 (2001).
4. H. Zeng, M. Zheng, R. Skomski, D.J. Sellmyer, Y. Liu, L. Menon and S. Bandyopadhyay, *J. Appl. Phys*., **87**, 4718 (2000).
5. K. Ounadjela, R. Ferré, L. Louail, J.M. George, J.L. Maurice, L. Piraux and S. Dubois, *J. Appl. Phys*., **81**, 5455 (1997).
6. T.G. Sorop, C. Untiedt, F. Luis, M. Kröll, M. Rasa and L.J. de Jongh, *Phys. Rev. B*, **67**, 014402 (2003).
7. R. Ferré, K. Ounadjela, J.M. George, L. Piraux and S. Dubois, *Phys. Rev. B*, **56**, 14066 (1997).
8. G.H. Lee, S.H. Huh, J.W. Park, H.-C. Ri, and J.W. Jeong, *J. Phys. Chem. B*, **106**, 2123 (2001).
9. J. Jorritsma and J.A. Mydosh, *J. Appl. Phys*., **84**, 901 (1998).
10. H. Zeng, S. Michalski, R.D. Kirby, D.J. Sellmyer, L. Menon and S. Bandyopadhyay, *J. Phys. Condens*., **14**, 715 (2002).
11. S. Kato, H. Kitazawa and G. Kido, *J. Magn. Magn. Mater*., **272-276**, 1666 (2004).
12. S. Dubois, J. Colin, J.L. Duvail and L. Piraux, *Phys. Rev. B*, **61**, 14315 (2000).
13. Introduction to Magnetic Materials, B. D Cullity, Addison-Wesley, MA, Chap. 11 (1972).
14. H. Masuda and M. Sato, *Jpn. Appl. Phys. (Berl.)*, **35**, L126 (1996).
15. K. Nielsch, F. Müller, A.-P. Li and U. Gösele, *Adv. Mater*., **12**, 582 (2000).